Complete Fermi Surface Mapping of $Bi_2Sr_2CaCu_2O_{8+x}$ (001): Coexistence of Short Range Antiferromagnetic Correlations and Metallicity in the Same Phase

P. Aebi, J. Osterwalder, P. Schwaller, and L. Schlapbach
Institut de Physique, Université de Fribourg, CH-1700 Fribourg, Switzerland

M. Shimoda,
National Research Institute of Metals, 2-3-12, Nakameguro, Meguro-Ku, Tokyo 153, Japan

T. Mochiku, and K. Kadowaki
National Research Institute of Metals, 1-2-2, Sengen, Tsukuba, Ibaraki 305, Japan
(Received 19 January 1994)

The Fermi surface of $Bi_2Sr_2CaCu_2O_{8+x}$(001) has been mapped at nearly 6000 points in **k** space using angle-resolved photoemission at 300 K. We observe both, features that are in good agreement with the local density calculation of Massidda, Yu, and Freeman [Physica (Amsterdam) **158C**, 251 (1988)] and others that are missing in the calculation. Among those missing, most importantly, we find a $c(2\times2)$ superstructure on the Fermi surface strongly suggesting short range antiferromagnetic correlations. It is remarkable that this is evident in the metallic state and in the Fermi surface itself.

PACS numbers: 71.25.Hc, 74.72.Hs, 79.60.Bm

Despite a large amount of experimental data on the electronic structure of high T_c materials the mechanism leading to high T_c superconductivity is not yet clear. More experiments are necessary either to remove controversy or to bring new or overseen features into evidence. In this process the Fermi surface (FS) of the normal, metallic state plays a key role and a microscopic theory certainly involves the understanding of its topology. We therefore present a complete mapping of the FS of $Bi_2Sr_2CaCu_2O_{8+x}$(001) [Bi(2212)], measured at 300 K.

For the investigation of the FS of a quasi-two-dimensional system with angular-resolved ultraviolet photoelectron spectroscopy (ARUPS), commonly, energy distribution curves (EDC's) are measured for different angles in order to determine the wave vector component parallel to the surface ($\mathbf{k}_\parallel$) where bands cross the Fermi level [1,2]. This tedious procedure bears the danger of missing important transitions since only a part of the Brillouin zone (BZ) is mapped. Recently, Santoni *et al.* [3] used an alternative way to obtain the same information. With a two-dimensional display-type analyzer they mapped the FS of layered graphite directly by measuring the total intensity within a narrow energy window at the Fermi energy (E_F). Clearly, high intensities are recorded at $\mathbf{k}_\parallel$ locations where direct transitions disperse through the energy window.

In the present work we adopted a similar procedure, using sequential angle-scanning data acquisition [4], to map photoemission intensities within a narrow energy window at E_F. Very recently we demonstrated the efficiency of this method by measuring cuts through the three-dimensional FS of Cu [5]. The obvious advantage of this procedure is that it provides a very accurate intensity mapping with a selectable uniform point density, covering at least the whole BZ. In contrast to conventional methods measuring complete EDC's, but at much fewer locations in the BZ, the present measurement will not miss any direct transitions crossing E_F.

Furthermore, displaying the data in a grey scale representation will accentuate faint features which otherwise would have been overseen.

The measurements were performed in a VG ESCA LAB Mark II spectrometer modified in order to enable motorized sequential angle-scanning data acquisition [4]. Photoelectrons excited with HeI (21.2 eV) radiation were analyzed with a 150 mm radius hemispherical analyzer operating with an angular resolution of 1° full cone and a pass energy of 1 eV corresponding to an energy resolution of about 30–40 meV. The base pressure was 2×10^{-11} mbar and the He partial pressure during operation of the differentially pumped He discharge lamp reached 1×10^{-8} mbar. Clean Bi(2212) surfaces were prepared by scotch tape cleaving at pressures in the low 10^{-10} mbar range. Samples were cleaved at room temperature and several tries were necessary to obtain a surface showing dispersion in ARUPS. Such a surface was stable for several weeks and did not deteriorate after x-ray (Mg $K\alpha$) irradiation and electron bombardment during low energy electron diffraction (LEED) analysis. The E_F scans involve 5993 different angular settings with a precision of better than 0.1°. The typical measuring time was 12 h. The data presented in this work have not been symmetry averaged. A small background due to the contribution of satellites of the HeI radiation has been subtracted mainly for presentation purposes. All the features discussed below are also visible without background subtraction. The crystal growth is described elsewhere [6].

In Fig. 1(a) we present the $\mathbf{k}_\parallel$ mapping of the intensity of HeI excited photoelectrons measured within a 10 meV wide energy window centered at E_F. High intensities re-

0031-9007/94/72(17)/2757(4)$06.00

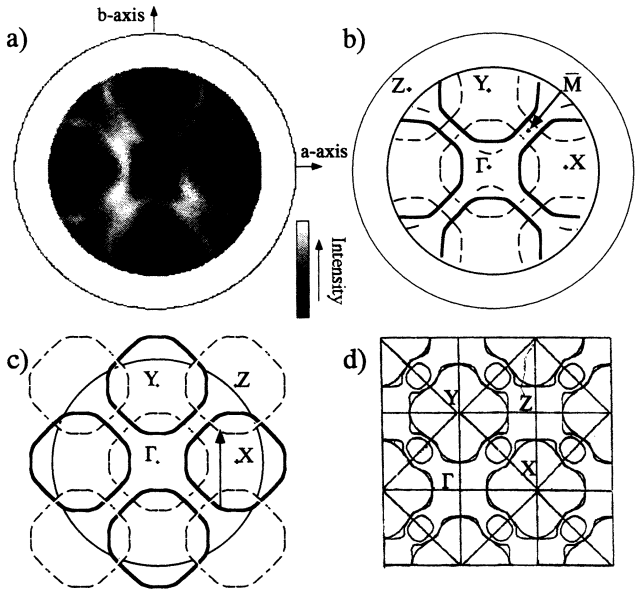

FIG. 1. (a) $\mathbf{k}_\parallel$ mapping of the intensity of He I (21.2 eV) excited photoelectrons collected within an energy window of 10 meV width centered at E_F. A logarithmic intensity scale is used to enhance weaker features. The outer circle indicates an emission angle of 90°. (b) Outline of (a), emphasizing the fine lines observed in the measurement and distinguishing between the stronger (thick lines) and weaker (dashed lines) sets of lines. (c) Taking the stronger set of lines in an extended zone scheme and superposing it on the original set with a shift of ΓY reproduces the pattern of (b) respectively (a). The circle indicates the range mapped by the experiment. (d) For comparison, the calculated FS of Ref. [7] using the FLAPW method.

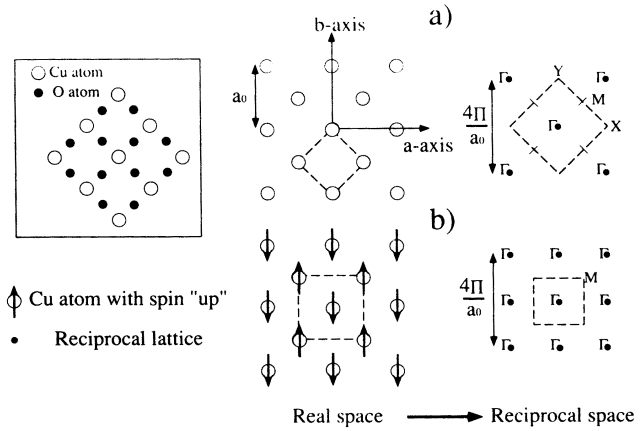

FIG. 2. Real space to reciprocal space transformation (a) for an ordinary Cu-O layer and (b) for a layer with AF spin correlations. The O atoms are neglected for clarity. Note that for a truly two-dimensional system Γ is equivalent to Z. The inset shows a real space lattice including the O atoms.

sult at $\mathbf{k}_\parallel$ locations where transitions move through E_F. These locations present themselves as relatively fine, well defined lines as pointed out in Fig. 1(b). Since the photoemission process conserves $\mathbf{k}_\parallel$, these lines correspond to a section through the FS as has been demonstrated in [5] for the example of Cu. Notice that for a truly two-dimensional system we can neglect the influence of $\mathbf{k}_\perp$ on this section. Furthermore, Γ and Z points of the reciprocal space of the face centered orthorhombic unit cell of Bi(2212) become equivalent.

We distinguish two sets of lines in Fig. 1(a), one type being strong and continuous and the other being weaker [see Fig. 1(b) as a guide to the eye]. It appears that a displacement of the strong set of lines of the FS by vectors ΓX or ΓY covers the set of weaker lines. This is illustrated in Fig. 1(c). In Fig. 1(d) we reproduce the calculated FS of Massidda, Yu, and Freeman [7] using the full-potential linearized augmented plane wave (FLAPW) method. Common features as well as differences are present. Excellent agreement exists for the distance between Γ and the crossings of the FS in the direction of X and Y and the curvature of some of their bands of the FS near these crossings. Discrepancies around $\bar{M}$ are evident and of course the set of weaker lines is completely missing in the calculation. The present FS measurement differs considerably from that of Ref. [2], probably due to their much lower point density and their procedure to extract FS crossings from the EDC's.

The difference between X and Y is given by the slightly different values for the lattice parameters a and b and the incommensurate modulation of the crystal in the direction of b [8]. We have independently determined the a and b directions by LEED and photoelectron diffraction [9]. For states at the Fermi level in Fig. 1(a) we only see a small difference in the brightness of the curved lines near Γ, being weaker in the b direction. Another feature connected to the b direction are two faint lines, roughly parallel to a and very close to the Γ point. One of the two lines also appears near the Z points at the very border of the measurement, the other remaining outside. For other constant energy surfaces below the Fermi level, however, the anisotropy between the a and b directions becomes very strong (not shown).

We can reproduce the experimental FS of Fig. 1(a) in an extended zone scheme by superposing the FS centered at Γ (strong lines) with its replica centered at X or Y (weak lines) as shown in Fig. 1(c). Just as in a LEED experiment, the resulting new periodicity, which is $c(2\times2)$, must be associated with a larger unit cell in real space, as is explained in Fig. 2. We consider the two-dimensional system of the Cu-O layer (inset). This is where the states at the Fermi level are located mainly. For clarity we only draw the square lattice of the Cu atoms neglecting O atoms. In Fig. 2(a) we illustrate the transformation of the ordinary real space lattice into reciprocal space. If, however, the Cu lattice is occupied with antiferromagnetically (AF) correlated spins [Fig. 2(b)], we notice that additional Γ points appear at the

former X and Y locations. Therefore, by symmetry, AF correlation will reproduce the same FS around X or Y as it does around Γ, no matter how this correlation affects the electronic structure. Relative intensities will depend on the strength of the exchange scattering [10] at E_F, and on the degree of AF correlation. Of course, a $c(2\times2)$ atomic rearrangement of the real space lattice would have the same effect in reciprocal space but this is unlikely to happen since the Cu-O layer is well below the surface (the cleavage plane is between the Bi-O layers [9]) and we are not aware of any other experimental reports supporting such an atomic rearrangement in the bulk of Bi(2212). LEED and scanning tunneling microscopy [11] do not give any indication of such a reconstruction at the surface. We observe a quite sharp quasi-(5×1) pattern [12] due to the incommensurate modulation along the b direction.

In order to corroborate the $c(2\times2)$ superstructure on the FS we measured other constant energy surfaces for energies slightly below E_F using the same measuring procedure. Different sets of lines contributing to the FS should disperse differently depending on the reciprocal lattice point they are centered around. Figure 3(a) shows the intensity distribution along X-Γ-X for E_F, i.e., a cut through a map as presented in Fig. 1(a), and for several binding energies up to 400 meV. The dispersion of the intensity maxima clearly indicates that the "squarelike" pattern centered around Γ [see Fig. 1(a)] contracts with increasing binding energy consistent with the band structure calculation of Massidda, Yu, and Freeman [7]. If the weaker set of lines in Fig. 1(a), centered at X or Y, is symmetry related to the pattern around Γ, as outlined in terms of AF correlations above, then these lines should also contract around X or Y with increasing binding energy. Cuts through the constant energy surfaces along Z-Y-Z in Fig. 3(b) clearly confirm this behavior. The asymmetry in absolute intensities observed around Y arises from the rotation of the polarization plane defined by the direction of incidence of the unpolarized He light source as we rotate the sample [5].

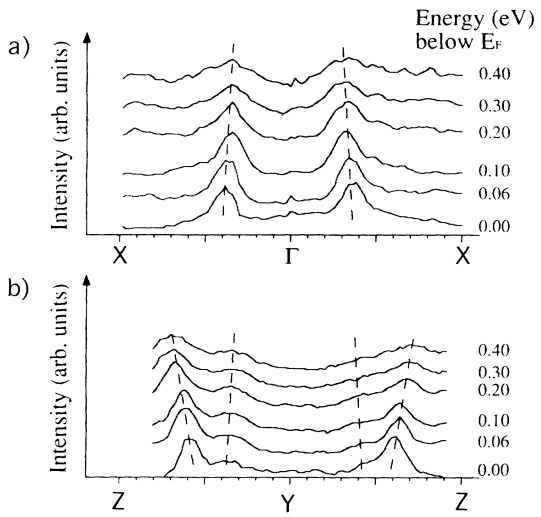

FIG. 3. Intensity distribution for cuts through the constant energy surface maps (a) along X-Γ-X and (b) along Z-Y-Z for E_F and several binding energies. The asymmetry around Y is due to the polarization, breaking the mirror symmetry of the experiment. Note the analogous behavior of the symmetry related maxima in (a) and (b).

A characteristic feature of the FS [Fig. 1(a)] is the high state density around the $\bar{M}$ point. FLAPW calculations of the FS [7] predict a small electron surface from Bi-O derived bands. Two almost degenerate, very flat bands from even and odd combinations of the two Cu-O planes are proposed from photoemission experiments [2]. From our experiment, however, it appears that this high state density region around $\bar{M}$ simply occurs due to the crossing of the different parts of the FS according to Fig. 1(c). We have no evidence for the Bi-O electron pocket.

There has been considerable discussion on FS nesting [2,7]. This discussion is important concerning an eventual explanation of the strongly peaked dynamical susceptibility near $(\pi/a,\pi/a)$ [13], a being the Cu-Cu nearest neighbor distance. Since the vector $(\pi/a,\pi/a)$ corresponds to the vector ΓY and the "AF" FS can be obtained by superposing the stronger set of lines of Fig. 1(b) with its replica translated by ΓY [see Fig. 1(c)], short range AF spin correlations present an alternative explanation [14].

How does our observation of a superstructure on the FS fit into the general picture we have of doped cuprates? Neutron scattering studies showed AF spin correlations in insulating, metallic, and superconducting $La_{2-x}Sr_x$-CuO_4 [15] and YBaCuO [16] with a correlation length depending on the doping and becoming as small as 10 Å for high doping. ARUPS has a coherence length of this order of magnitude and is thus sensitive to such correlations. LEED, however, does not give any indication, even though it can see AF ordering in principle [17]. This either means that the Cu-O layers are buried too deeply within the surface to contribute or, more probably, that the coherence length of the ordering is shorter than the $\sim$100 Å requested for LEED.

In summary, we have presented the first complete FS mapping for Bi(2212). A $c(2\times2)$ superstructure appears on the FS strongly suggesting local AF spin correlations in the metallic phase. We do not observe the Bi-O derived electron pockets at the $\bar{M}$ point [7] and the FS exhibits only a weak perturbation due to the modulation along b. Both facts indicate a highly two-dimensional character of the states at E_F.

The authors are indebted to S. Hüfner for suggesting this experiment. We wish to thank G. A. Sawatzky for critical reading of the manuscript and D. Baeriswyl, K. A. Müller, R. Leckey, R. Fasel, and T. Kreutz for many stimulating discussions. Skillful technical assistance was provided by E. Mooser, O. Raetzo, and H. Tschopp. This project has been supported by the NFP30.

[1] R. H. Gaylord, K. H. Jeong, and S. D. Kevan, Phys. Rev. Lett. **62**, 2036 (1989); S. G. Kevan, Phys. Scr. **T31**, 32 (1990); C. G. Olson, R. Liu, D. W. Lynch, R. S. List, A. J. Arko, B. W. Veal, Y. C. Chang, P. Z. Jiang, and A. P. Paulikas, Phys. Rev. B **42**, 381 (1990).

[2] D. S. Dessau, Z.-Z. Shen, D. M. King, D. S. Marshall, L. W. Lombardo, P. H. Dickinson, A. G. Loeser, J. DiCarlo, C.-H. Park, A. Kapitulnik, and W. E. Spicer, Phys. Rev. Lett. **71**, 2781 (1993).

[3] A. Santoni, L. J. Terminello, F. J. Himpsel, and T. Takahashi, Appl. Phys. A **52**, 229 (1991).

[4] J. Osterwalder, T. Greber, A. Stuck, and L. Schlapbach, Phys. Rev. B **44**, 13764 (1991); D. Naumović, A. Stuck, T. Greber, J. Osterwalder, and L. Schlapbach, Phys. Rev. B **47**, 7462 (1993).

[5] P. Aebi, J. Osterwalder, R. Fasel, D. Naumović, and L. Schlapbach, Surf. Sci. (to be published).

[6] T. Mochiku and K. Kadowaki, in *Electronic Properties and Mechanisms of High Tc Superconductors,* edited by T. Oguchi, K. Kadowaki, and T. Sasaki (Elsevier Science, New York, 1992); in Proceedings of the IUMRS-ICAM-93, Tokyo, 1993 (Elsevier, New York, to be published).

[7] S. Massidda, Jaejun Yu, and A. J. Freeman, Physica (Amsterdam) **158C**, 251 (1988).

[8] A. Yamamoto, M. Onoda, E. Takayama-Muromachi, F. Izumi, T. Ishigaki, and H. Asano, Phys. Rev. B **42**, 4228 (1990).

[9] M. Shimoda, T. Greber, J. Osterwalder, and L. Schlapbach, Physica (Amsterdam) **196C**, 236 (1992).

[10] R. E. DeWames and L. A. Vredevoe, Phys. Rev. Lett. **18**, 853 (1967).

[11] C. K. Shih, R. M. Feenstra, J. R. Kirtley, and G. V. Chandrashekhar, Phys. Rev. B **40**, 2682 (1989); C. K. Shih, R. M. Feenstra, and G. V. Chandrashekhar, Phys. Rev. B **43**, 7913 (1991); Xian Liang Wu, Yue Li Wang, Zhe Zhang, and Charles M. Lieber, Phys. Rev. B **43**, 8729 (1991).

[12] R. Claessen, R. Manzke, H. Carstensen, B. Burandt, T. Buslaps, M. Skibowski, and J. Fink, Phys. Rev. B **39**, 7316 (1989).

[13] J. Ruvalds and A. Virosztek, Phys. Rev. B **43**, 5498 (1991).

[14] D. J. Scalapino, E. Loh, Jr., and J. E. Hirsch, Phys. Rev. B **34**, 8190 (1986); J. E. Hirsch, Phys. Rev. Lett. **59**, 228 (1987); P. Monthoux and D. Pines, Phys. Rev. Lett. **69**, 961 (1992).

[15] R. J. Birgeneau, D. R. Gabbe, H. P. Jenssen, M. A. Kastner, P. J. Picone, T. R. Thurston, G. Shirane, Y. Endoh, M. Sato, K. Yamada, Y. Hidaka, M. Oda, Y. Enomoto, M. Suzuki, and T. Murakami, Phys. Rev. B **38**, 6614 (1988).

[16] J. M. Tranquada, P. M. Gehring, G. Shirane, S. Shamoto, and M. Sato, Phys. Rev. B **46**, 5561 (1992).

[17] P. W. Palmberg, R. E. DeWames, and L. A. Vredevoe, Phys. Rev. Lett. **21**, 682 (1968).

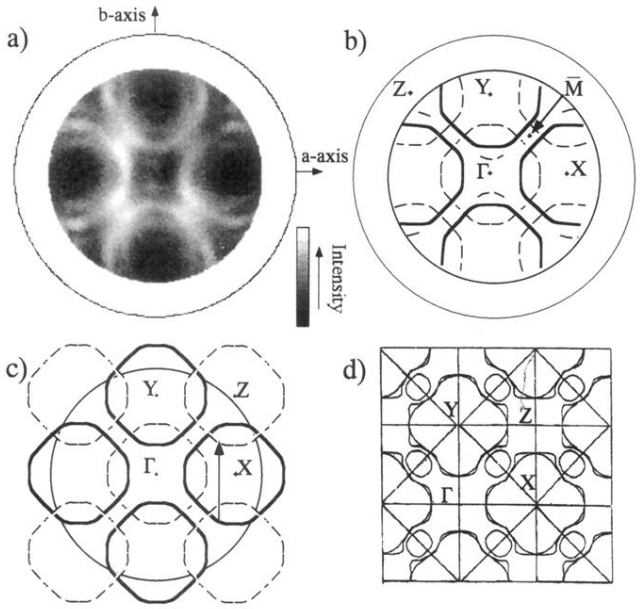

FIG. 1. (a) $\mathbf{k}_{\parallel}$ mapping of the intensity of He I (21.2 eV) excited photoelectrons collected within an energy window of 10 meV width centered at E_F. A logarithmic intensity scale is used to enhance weaker features. The outer circle indicates an emission angle of 90°. (b) Outline of (a), emphasizing the fine lines observed in the measurement and distinguishing between the stronger (thick lines) and weaker (dashed lines) sets of lines. (c) Taking the stronger set of lines in an extended zone scheme and superposing it on the original set with a shift of ΓY reproduces the pattern of (b) respectively (a). The circle indicates the range mapped by the experiment. (d) For comparison, the calculated FS of Ref. [7] using the FLAPW method.